



Universiteit
Leiden
The Netherlands

Inhibitors and activity-based probes for β -D-glucuronidases, heparanases and β -L-arabinofuranosidases

Borlandelli, V.

Citation

Borlandelli, V. (2023, October 24). *Inhibitors and activity-based probes for β -D-glucuronidases, heparanases and β -L-arabinofuranosidases*. Retrieved from <https://hdl.handle.net/1887/3645862>

Version: Publisher's Version

License: [Licence agreement concerning inclusion of doctoral thesis in the Institutional Repository of the University of Leiden](#)

Downloaded from: <https://hdl.handle.net/1887/3645862>

Note: To cite this publication please use the final published version (if applicable).

3

Synthesis and Biochemical Evaluation of a New Generation of Mechanism-based Heparanase Inhibitors

3.1 Introduction

Rational design of glycomimetics may yield compounds with improved pharmacokinetic and pharmacodynamic properties compared to native carbohydrate structures, which typically provide exquisite recognition substrates for carbohydrate-binding clinical targets.¹ Such glycomimetic designs have found successful application in the targeting of a number of lectins²⁻³ and glycan-processing enzymes⁴⁻⁷, as well as in the development of carbohydrate-based vaccines.⁸ Among the spectrum of glycomimetic designs, mimicry and stabilisation of the glycosidic bond offers the opportunity to reduce metabolic degradation, for instance by yielding inhibitors of retaining *endo*-acting glycosidases that are not hydrolysed by *exo*-acting ones. A case in point and subject of the studies described in this chapter are heparanase (HPSE) inhibitors whose design is based on the natural HPSE substrate, heparan sulfate (HS). HPSE is extensively studied as prospective pharmacological target for a wide range of human pathologies, including cancer, diabetic nephropathy and amyloidosis.⁹⁻¹⁰ As described earlier in this thesis, current pharmacochemical strategies have not met the need for HPSE-targeted therapies. The underlying complexity of targeting HPSE for therapeutic purposes can be ascribed to the lack of drug-like properties and stability of most HPSE binders¹⁰ and to the interplay between HS-degrading HPSE and its enzymatically-inactive homolog heparanase-2 (Hpa-2),¹¹ an endogenous inactivator of HPSE displaying apparent 10-fold greater binding affinity for HS than HPSE. Whilst the role of Hpa-2 in human pathophysiology has not been fully elucidated, a significant body of evidence points to the inhibition of HPSE activity as viable anti-metastatic cancer strategy.¹²⁻¹³ The enzyme possesses a well-characterised binding site and endogenous ligand, and therefore is amenable to traditional structure-based drug design approaches. In the context of HPSE drug design, the high degree of stereochemical information and the number of H-bond donating hydroxyl moieties confer indisputably to the superior binding affinity of carbohydrate-like scaffolds, which is difficult to reproduce with non-sugar fragments (see also Chapter 2). The considerations above might explain why distinct heparin and HS derivatives – in contrast to non-sugar structures – have progressed into clinical trials for the treatment of different malignancies.¹⁴⁻¹⁸ Clinical studies however have been hampered by the broad off-target profile and multiple modes of action of these large and heterogeneous structures, including anti-coagulation activity, anti-inflammatory and immunomodulatory properties.¹⁹⁻²⁰ This opens an avenue for reducing cross-reactivity by tailoring the saccharidic structure and biochemical information of endogenous ligand heparan sulfate (HS) with glycomimetic designs. Recent research on HPSE drug design has demonstrated that a set of

pseudo-disaccharidic glucuronic cyclophellitols²¹ – to which class compound **1** belongs – serves as potent and selective mechanism-based HPSE inactivators. However, monosaccharidic glucuronic cyclophellitols²², as holds true for uronic acid-type iminosugars²³⁻²⁴, have poor HPSE selectivity. Undesired targets of such small-molecule HPSE binders are retaining *exo*- β -D-glucuronidases, found as isozymes in blood plasma²⁵ and lysosomes²⁶ and as microbial enzymes²⁷⁻²⁸ secreted by the human gut microbiome in the human gastrointestinal tract. The physiological occurrence of *exo*- β -D-glucuronidases suggests that orally- or intravenously-administered small-molecule HPSE inhibitors able to engage with *exo*- β -D-glucuronidases would possibly suffer from toxicity and reduced bioavailability. One strategy to circumvent *exo*- β -D-glucuronidase engagement is exemplified by the development of 4-*O*-modified glucuronic cyclophellitols as described in Chapter 2 of this thesis. Furthermore, the presence of the α -(1,4)-glycosidic bond linking GlcNAc to glucuronic cyclophellitols in **1** and congeners points to *exo*- α -glycosidases such as inverting and/or retaining α -hexosaminidases as putative off-targets, as illustrated in Figure 3.1. This consideration may hold true for oligosaccharidic competitive HPSE inhibitors, which typically possess one or more α -(1,4)-bonds linking GlcNAc/GlcNS to uronic acid GlcUA/IdoA. Modification of the glycosidic bond with a glycosidase-resistant isoster may reduce the number of off-targets while simultaneously increasing the stability of glycomimetics in acidic medium present in the gastrointestinal tract, and reducing hydrophilicity. Mimicry and stabilisation of the glycosidic bond has traditionally been sought for by substitution of the anomeric oxygen with carbon (*C*-glycosides)²⁹⁻³¹ or with the heteroatoms S and Se (*S*-glycosides³² and *Se*-glycosides³³ respectively). This approach abolishes the anomeric effect and imparts enhanced metabolic and hydrolytic stability, yet it can significantly change the flexibility and length of inter-glycosidic linkages, as well as the ligand conformation and spatial occupation of the binding site. These changes might result in elevated entropic penalties for protein binding. An alternative strategy would entail incorporation of heteroatoms³⁴⁻³⁵ or a methylene group³⁶⁻³⁷ in place of the endocyclic oxygen. This modality, especially when a methylene moiety is used, generally leads to minor changes in the conformational landscape compared to exocyclic oxygen replacement approaches, thus allowing to retain most of the network of non-covalent ligand-protein interactions and to potentially reduce entropic losses in binding. Interestingly, both exocyclic and endocyclic oxygen mimicry designs are not documented in the field of HPSE drug design.

Expanding on the results described in Chapter 2 of this thesis and in line with previous work on mechanism-based HS-mimicking disaccharide cyclophellitols²¹ and *endo*-glycosidase

inhibitors,³⁷ a pseudo-saccharidic unit at the 4-*O* position of glucuronic cyclophellitol (**2**, Figure 3.2) is expected to provide enhanced binding affinity and ligand occupancy of the -2 HPSE subsite compared with recently published 4-*O* alkyl modifications.

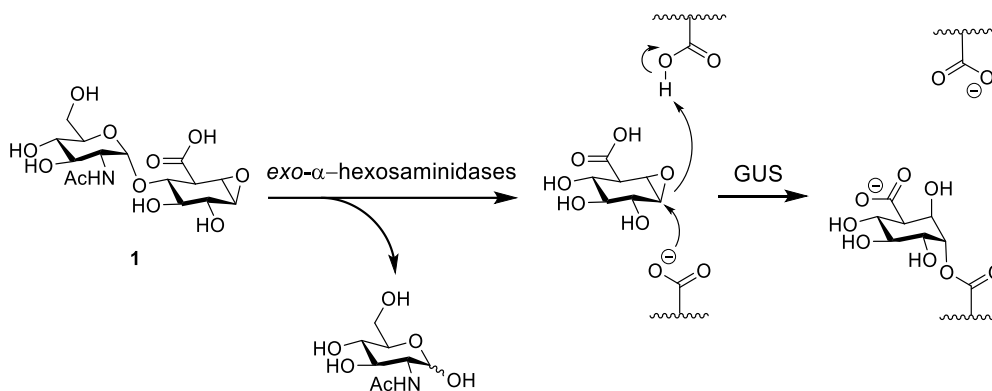


Figure 3.1. Putative degradation of **1** by retaining and/or inverting *exo*- α -hexosaminidases, with the resulting liberated glucuronic cyclophellitol available for retaining *exo*- β -D-glucuronidase (GUS) inhibition.

To stabilise the inhibitor against *exo*-glycosidases, substitution of the endocyclic oxygen in **1** with a methylene moiety was considered to afford in effect a dicarbasugar entity. Furthermore, it was reasoned that substitution of the 2'-*N*-Ac moiety with a secondary hydroxy group would allow to retain most H-bond interactions while reducing the synthetic complexity based on precedent unpublished work. In this chapter, the synthesis of compound **2** is described, along with the preparation of non-carba-disaccharidic analogue **3**. Both compounds were then assessed on their ability to inhibit recombinant HPSE and on their HPSE-GUSB inhibitory potency in platelet extracts in comparison to parent compound **1**.

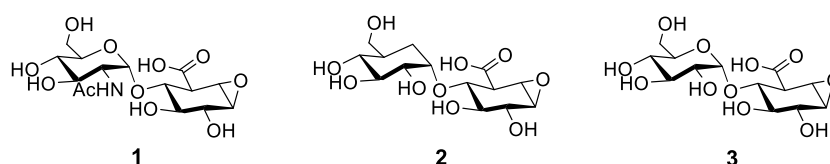
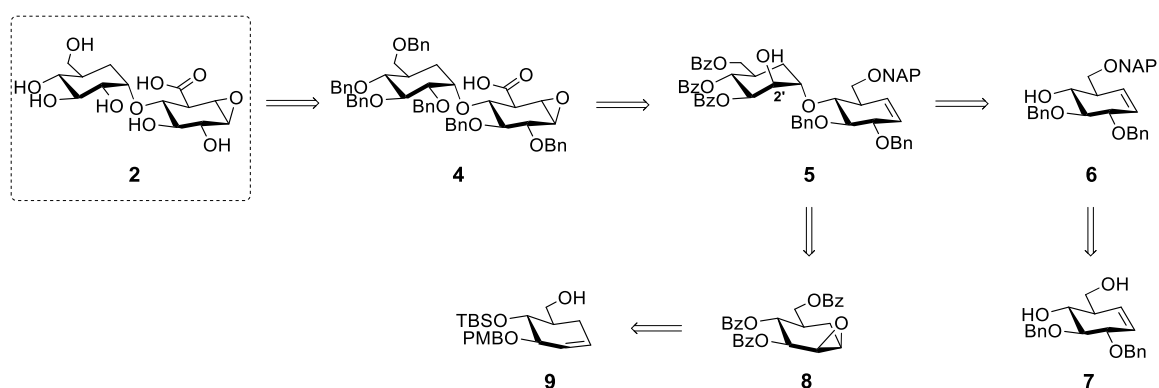


Figure 3.2. Structures of proposed stabilised HPSE mechanism-based inhibitor **2** and non-hydrolytically-stable disaccharidic congeners **1**²¹ and **3**, evaluated *in vitro* in this Chapter.

In a retrosynthetic analysis, target compound **2** can be derived from per-benzylated intermediate **4** which in turn would emerge after protecting group manipulation and inversion of configuration of the 2' position in cyclohexene **5** (Scheme 3.1). The latter can be formed by Lewis acid-mediated epoxide ring opening of precursor **7** in the presence of excessive amount of orthogonally-protected cyclohexene **6**, which can be obtained in gram-scale according to published procedures in multiple steps.³⁸ The epoxide-based pseudo-glycosyl donor **8** is

accessed by protecting group manipulation of carba-sugar **9**.³⁹ Analogous to the concept of disarming glycosidic donors in conventional glycosylation methodologies,⁴⁰ it was anticipated that installation of multiple benzoyl groups in **9** would reduce the electron density of the correspondent epoxide-based pseudo-glycosidic donor **9** and thereby increase its electrophilic reactivity towards nucleophile **6**. The use of the benzoyl ester protecting group was sought to enable facile interchange of protecting groups during the synthesis scheme. In the following sections, the synthesis and biological assessment of mechanism-based HPSE inactivator **2** is presented. Its *in vitro* evaluation is performed with the use of recently published ABPs, and the inhibitory potency against *endo*- β -D-glucuronidases is compared with previous best-in-class mechanism-based inhibitor **1**²¹ as well as with its hydrolysable disaccharidic analogue **3**.



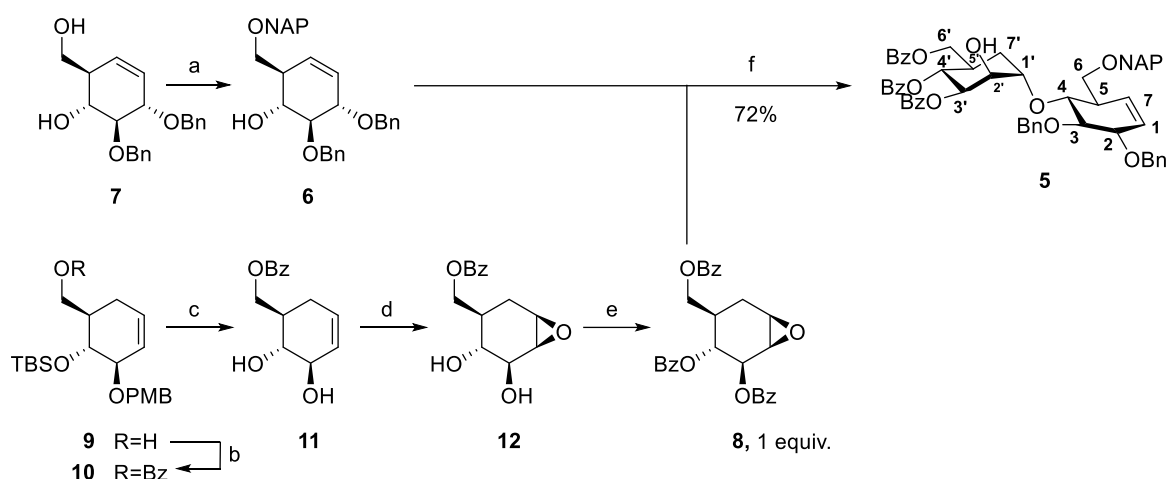
Scheme 3.1. Retrosynthetic analysis of the proposed HPSE inhibitor **2** disclosed in this chapter.

3.2 Results and discussion

3.2.1 Synthesis of mechanism-based HPSE inhibitor **2**

Synthetic accessibility of mechanism-based HPSE inhibitor **2** is provided by BF_3 -mediated epoxide ring opening of perbenzoylated *epi*-1,2-carba-manno-cyclophellitol **8** with an excess of NAP-protected benzylated *gluco*-cyclohexene **6** as illustrated in Scheme 3.2. This synthetic methodology, which will be referred to as ‘pseudo-glycosylation’ hereafter, was conceived to reproduce the α -1,4-selectivity of a conventional glycosylation, but performed with carbasaccharidic equivalents of a glycosyl donor (as per **8**) and glycosyl acceptor (as per **6**). Reactants **6** and **7** were prepared from precursors **7**³⁸ and **9**³⁹, respectively, both obtained according to precedent multi-step strategies. More specifically, pseudo-glycosyl donor **8** was obtained from orthogonally-protected carba-sugar **9** upon protecting group manipulation and epoxidation. Benzoylation of **9** was followed by step-wise removal of silyl ether and *p*-methoxybenzyloxy protecting groups which allowed facile deprotection of secondary hydroxyl functionalities, resulting in alcohol **11**. Absence of protecting groups at the allylic secondary

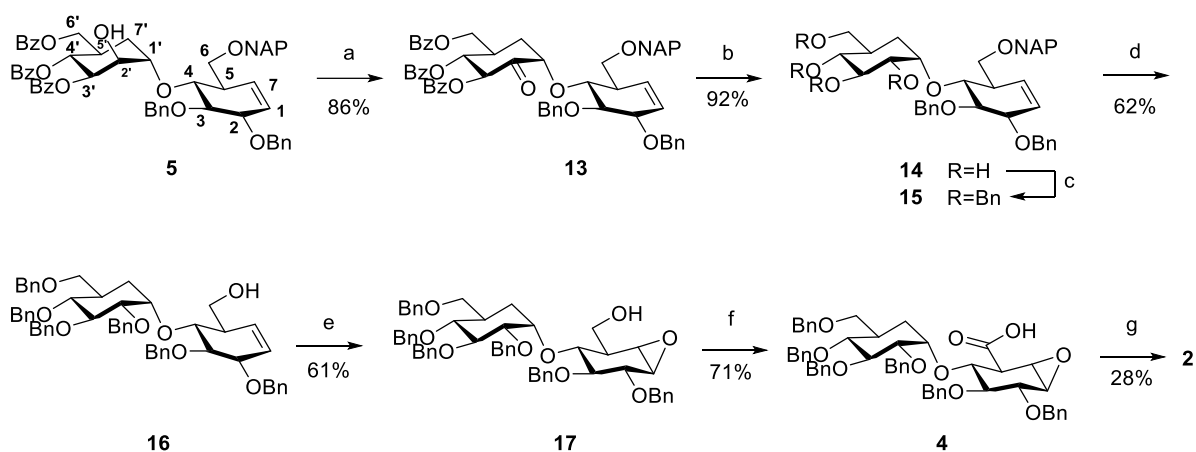
hydroxyl functionality was sought to direct the selectivity of the *m*-CPBA-mediated epoxidation in favour of the desired β -facial stereoselectivity. Having prepared the required pseudo-glycosidic donor and acceptors in gram-scale, pseudo-carbadiaccharidic intermediate **5** was then assembled. For the desired regioselectivity of the pseudo-glycosylation step, it was found that nucleophilic attack of epoxide **8** required excessive amount of *gluco*-configured pseudo-glycosyl acceptor **6** and sub-stoichiometric amount of the Lewis acid $\text{BF}_3\text{-OEt}_2$. In line with expectations, yields of the pseudo-glycosylation step could be further improved by employing a perbenzoylated pseudo-glycosidic donor in place of more electron-rich scaffolds as NAP- or Bn-protected variants. This choice of protecting group significantly simplified silica gel chromatographic separation of desired product **5** from excessive unreacted cyclohexene **6**: in previous attempts, the similarity in polarity between **6** and the pernapthylated equivalent of **5** required a two-step purification involving silica gel chromatography followed by size-exclusion chromatography.



Scheme 3.2. Reagents and conditions: (a) i. NapBr, KI, K_2CO_3 , 2-aminoethyl-diphenylborate, CH_3CN , 88%. (b) BzCl, py, DCM, 95%. (c) i. TBAF, THF; ii. DDQ, DCM/phosphate buffer, dark, 79% over 2 steps. (d) *m*-CPBA, DCM, 0°C , 67%. (e) BzCl, pyridine, 0°C , 84%. (f) $\text{BF}_3\text{-OEt}_2$ (0.5 eq), 4 (eq), DCM, $0^\circ\text{C} \rightarrow \text{rt}$, 18 h, 75%.

With the pseudo-disaccharidic intermediate **5** in hand (Scheme 3.3), the configuration of the axial $2'$ -hydroxy group was inverted to yield equatorial $2'$ -epimeric intermediate **14** after Dess-Martin oxidation and subsequent one-pot thermally-controlled debenzoylation and ketone reduction with NaBH_4 . In particular, controlled increase in temperature from -60°C to 0°C over 4 hours during the ketone reduction step was found fundamental in preventing epimerisation at the $1'$ -position while attaining removal of the benzoyl groups. Conversely, progressive temperature increase over a shorter time window resulted in one-pot

debenzoylation of **13** with concomitant isolation of the 1'-epimer of product **14**. Because of the intrinsic base-lability of glucuronic cyclophellitols, benzoyl deprotection methodologies are not feasible as final deprotection step of strained carboxylates. One-pot debenzylation proved therefore advantageous during the synthesis: the partially unprotected polyhydroxylated pseudo-disaccharide **14** was perbenzylated, to introduce hydrogenolytically-labile protecting groups amenable to deprotection of glucuronic cyclophellitols. The following steps resemble the synthetic methodologies adopted at a late stage for the synthesis of 4-*O*-modified glucuronic cyclitols in Chapter 2. Specifically, denaphthylation of **15** with 2,3-dichloro-5,6-dicyano-1,4-benzoquinone (DDQ) in darkness enabled control over the stereoselectivity of the *m*-CPBA-mediated epoxidation. Next, Epp-Widlansky oxidation⁴¹ of primary alcohol **17** at 0 °C afforded carboxylate **4** in high yields. Lastly, global deprotection of late-stage intermediate by Pearlman's catalysed hydrogenolysis and reverse-phase HPLC purification resulted in final product **2** for subsequent *in vitro* studies.



Scheme 3.3. Reagents and conditions: (a) Dess-Martin, THF/MeOH, rt, 18 h, 86%. (b) NaBH₄, THF/MeOH, -60 °C → 0 °C, 4 h, then 0 °C for 18 h, 92%. (c) BnBr, NaH, DMF, 0 °C → rt, 73%. (d) DDQ, DCM/H₂O, 1.5 h, darkness, 58%. (e) *m*-CPBA, DCM, 4 °C, 18 h, 62%. (f) TEMPO/BAIB, DCM/^tBuOH/H₂O, 4 °C, 19 h, 71%. (g) Pd/C, H₂, MeOH/^tBuOH/dioxane, rt, 5 h, 31%.

3.2.2 *In vitro* inhibition of recombinant *endo*-β-D-glucuronidases

The inhibitory potency of newly synthesised candidate **2** was next assessed against recombinant *endo*-β-D-glucuronidase from *Acidobacterium capsulatum* (AcGH79) via in-gel competitive profiling using as fluorescent read-out Cy5-tagged β-D-glucuronidase ABP following the protocol as presented in chapter 2. In these experiments, cyclitol **2** displayed low micromolar inhibition of AcGH79 (apparent IC₅₀: 1.2 ± 0.3 μM, illustrated in Figure 3.3) at the

tested enzyme concentration, suggesting that **2** is able to block the *endo*-activity of AcGH79 at micromolar concentrations.

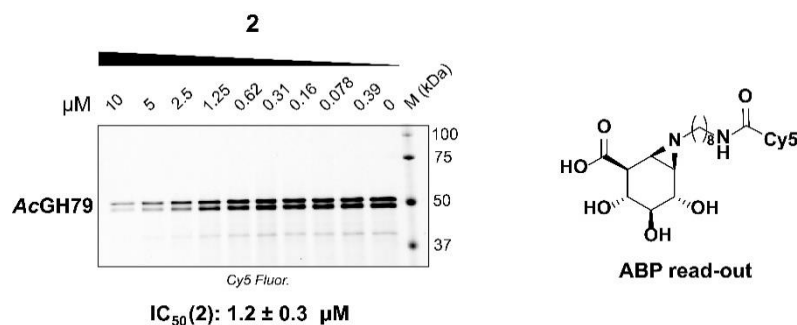


Figure 3.3. Assessment of inhibitory potency of **2** by Cy5-tagged β -D-glucuronidase ABP-based in-gel competitive profiling against recombinant AcGH79. Reported apparent IC_{50} value was calculated from a set of three replicates.

To gain insight into human HPSE structure-activity relationships, apparent HPSE inhibition was tested for cyclitol **2**, its disaccharidic analogue **3** (as synthesised by V. Lit) and parent HPSE inhibitor **1** (Figure 3.3). All tested compounds scored apparent HPSE IC_{50} values in the low to sub-micromolar range (Table 3.1). However, quantification of the bands led to IC_{50} values with large standard deviations. In an attempt to make a more accurate comparison, competitive ABPP gels with **1** versus **2**, and **1** versus **3** were performed (Figure 3.4). In these gels **2** clearly exhibited slightly lower inhibitory potency when compared with reference compound **1**, yet in the same sub-micromolar range. On the other hand, candidate **3** could inactivate HPSE down to 2 μ M inhibitor concentration similarly to its C-analogue analogue **2**. From the comparison of the observed apparent inhibitory potency of **1** and **3** against purified HPSE, it results that 2'-N-Ac group confers slightly higher binding affinity against the purified recombinant HPSE compared to 2'-OH functionality. Moreover, the collected evidence indicates that substitution of the endocyclic oxygen in **3** with a methylene group (as in **2**) does not impair binding affinity against purified HPSE.

Table 3.1. Apparent IC_{50} values for *in vitro* inhibition of HPSE by compounds **1**–**3**. Error ranges depict standard deviations from two technical replicates with rhHPSE, and from three technical replicates in platelet extracts.

<i>In vitro</i> IC_{50} (μ M)	1	2	3
rhHPSE ^a	0.3 \pm 0.2	0.5 \pm 0.5	1 \pm 1
HPSE (platelet) ^a	0.9 \pm 0.3	0.4 \pm 0.2	5 \pm 1

^a In-gel competitive ABPP-based assay

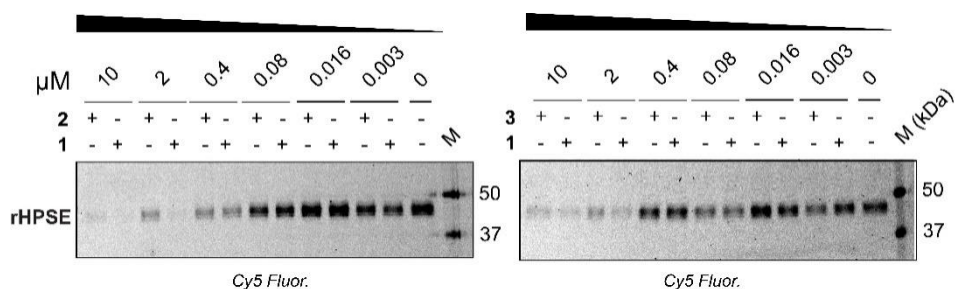


Figure 3.4. Assessment of inhibitory potency of **1-3** by Cy5-tagged β -D-glucuronidase ABP-based in-gel competitive profiling against recombinant human rhHPSE.

Together with previous reported work on disaccharidic glucuronic cyclophellitols,²¹ these results suggest that the HPSE -2 subsite can accommodate minor modifications of the 2' position provided that the electron density, the steric properties and the spatial occupancy are not drastically altered.

3.2.3 Inhibitory activity in blood platelet extracts

To assess HPSE selectivity over *exo*- β -D-glucuronidase of the newly designed inhibitor and to investigate its putative superior hydrolytic stability, complex biological samples were interrogated by in-gel apparent IC_{50} determination. Following the same criteria as described in Chapter 2, platelet extracts²¹ were chosen as preferred biological sample. Interestingly, the trend in apparent HPSE IC_{50} observed in platelet extracts differs from the one found with recombinant HPSE. As shown in Figure 3.4, preincubation with inhibitors **1-3** effectively abrogates HPSE signal down to 2.5-5 μ M inhibitor concentration without altering GUS signals. This demonstrates the inherent HPSE selectivity of newly synthesised **2** and **3** over *exo*-acting isoforms, confirming expectations. Moreover, candidate **2** scored a half order of magnitude lower apparent HPSE IC_{50} value (as in Table 3.1) compared to **1**²¹ and **3**, both of which inactivated HPSE with similar low micromolar inhibitory potency under the tested conditions. This major finding suggests that *exo*- α -glycosidases such as hexosaminidases present in platelet extracts might cleave the α -glycosidic linkage in **1** and **3**, thereby diminishing the inhibitory efficacy of the two latter compounds. It is worth noting that expression and concentration of HPSE in platelets differs between individuals, which might explain the higher IC_{50} value quantified for **1** in this assay in comparison to previous reports²¹ which made use of platelet extract from a different individual. Under the tested conditions mimicry of the endocyclic oxygen in **3** with a methylene group (as in **2**) affords superior HPSE inhibitory potency compared to substitution of Glc in **3** for GlcNAc (as in **1**) in platelet extracts. Taken together with the results disclosed in previous sections of this chapter, the observed IC_{50} value reported

for **2** in platelets can be arguably ascribed to an enhancement in metabolic stability rather than to an increase in HPSE binding affinity compared to precedent non-stabilised inhibitors. Future studies in platelet extracts as well as in liver and plasma microsomes are due to investigate this hypothesis further. Complementing the findings herein presented with the results from the docking analysis discussed in Chapter 2, it may be inferred that abolishing the anomeric effect by modification of the endocyclic oxygen in **3** with a methylene moiety (as in **2**) may not significantly alter the conformational landscape of the pseudo-saccharidic scaffold.

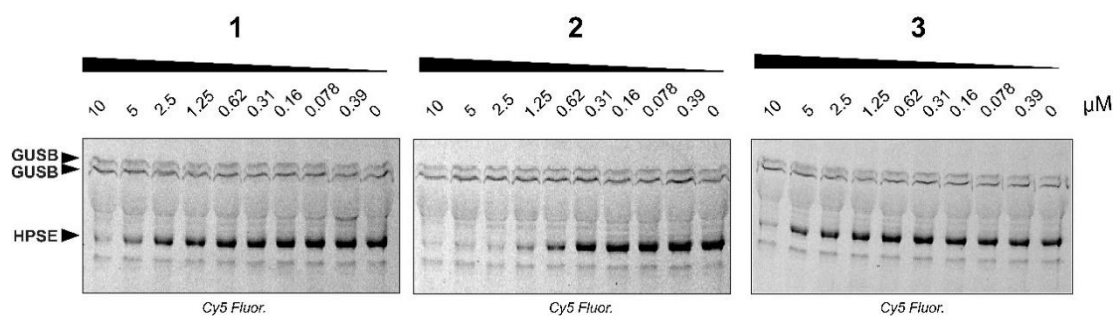


Figure 3.5. *In vitro* HPSE selectivity by **1-3** in platelet lysates as determined by competitive ABPP in blood platelet lysate. Fluorescent labelling of HPSE by β -D-glucuronidase ABP can be abrogated by pre-incubation with the tested inhibitors without altering GUSB signal, thus demonstrating their innate selectivity for human HPSE in the presence of *exo*-acting β -D-glucuronidase. In particular, **1** and **3** scored comparable apparent HPSE IC_{50} values. In contrast, **2** exhibited higher HPSE inhibitory potency.

3.3 Conclusions

Stabilised carba-disaccharidic HPSE binder **2** was synthesised from suitably protected carba-monosaccharidic precursors as described in this chapter. The synthesis relies on the Lewis-acid-mediated epoxide ring opening of a perbenzoylated pseudo-glycosyl donor, followed by subsequent protecting group manipulation and 2'-position modification. The multi-step synthesis was followed by *in vitro* assessment of **2** against recombinant *endo*-glucuronidase AcGH79. Comparative analysis of recombinant hHPSE inhibition by **2** with non-stabilised disaccharidic scaffolds **1** and **3** conducted with in-gel competitive fluorescent labelling assay proved that all tested compounds are competent low to sub-micromolar inactivators of rhHPSE. Biochemical evaluation of **2** in platelet extracts confirmed the inherent inhibitory selectivity for HPSE over *exo*-glucuronidase isoforms, and put to test the hydrolytic stability of the available scaffolds. From this assay, pseudo-disaccharide **2** was found to outperform disaccharidic analogue **3** and reference compound **1** in terms of apparent inhibitory efficacy, indicating a superior hydrolytic stability of glycomimetic **2** towards *exo*-acting glycosidases present in biological milieu.

Future studies may aim at investigating the biological origins of the reported HPSE IC₅₀ trend observed in platelet extracts, namely by blocking *exo-α*-hexosaminidase activity with a known inhibitor prior cABPP in platelet extracts. This is foreseen to shed light on the role of *exo-α*-hexosaminidases as putative off-targets of non-stabilised saccharidic scaffolds. Once the hydrolytic stability in platelets has been fully investigated, off-target profiling and metabolic stability in plasma and liver microsomes may be assessed as a next step.

3.4 Acknowledgements

Zachary Armstrong from Leiden University is kindly acknowledged for the protein expression and purification and for platelet preparation, as well as for valuable discussions regarding IC₅₀ determinations. Alberto Pettinari and Chucky Chau are acknowledged for their synthesis work in the context of their MSc internships. Yurong Chen, Sybrin Schröder, Ken Kok and Rob Lammers from Leiden University are kindly acknowledged for valuable discussions in the context of inhibitor synthesis. Sybrin Schröder is kindly acknowledged for previous unpublished work on the synthesis towards carba-disaccharidic HPSE inhibitors. Vincent Lit from Leiden University is kindly acknowledged for the synthesis of non-carba disaccharidic inhibitor **3**.

3.5 Experimental methods

3.5.1 Biochemical experiments

Materials

All chemicals were obtained from standard commercial sources. Low protein binding 0.5 mL Eppendorf tubes for use in the the *in vitro* biochemical evaluation were purchased from Merck Life Science NV.

Recombinant protein production and purification

HPSE – Human HPSE was expressed and purified according to previously reported procedures.⁴²

AcGH79 – AcGH79 was expressed and purified according to previously reported procedures.²¹

Harvested cells overexpressing HPSE or AcGH79 were resuspended in ~50 mL Histrap buffer (20 mM Tris pH 8.0, 500 mM NaCl, 20 mM imidazole, 1 mM DTT), supplemented with DNase I, and cOmplete™ EDTA protease inhibitors. Cells were lysed using a cell disruptor at 40 kPSI operating pressure, then lysate clarified by centrifugation at 40,000 g at 4 °C for 30 min. Clarified supernatant was loaded onto a 5 mL HisTrap FF crude column pre-equilibrated with HisTrap buffer A, washed with 10 CV of HisTrap buffer A, before eluting with HisTrap buffer B (20 mM Tris pH 8.0, 500 mM NaCl, 1 M imidazole, 1 mM DTT) over a 20 CV linear gradient. Concentrated protein was loaded onto a

Superdex S200 16/600 pg SEC column pre-equilibrated in SEC buffer (20 mM HEPES pH 7.4, 200 mM NaCl, 1 mM DTT). Purified protein was flash frozen in liquid N₂ and stored at -80 °C for use in further experiments.

Preparation of cell samples

Isolation of platelets from whole blood followed previous procedures.²¹ Approval for tissue collection was granted by the University of York medical ethics committee. Platelet lysates were prepared as previously described.²¹ Aliquots of lysates were flash frozen in liquid N₂, and stored at -80 °C until use.

Determination of *in vitro* apparent IC₅₀ values

AcGH79 – The *in vitro* apparent IC₅₀ value of **2** against recombinant AcGH79 was measured by in-gel competitive ABPP with ABP **7** (as described in Chapter 2) as fluorescent read-out. The enzymatic reactions were carried out at a constant concentration of enzyme (20 nM, final) and of read-out ABP **7** (100 nM, final). For inhibitor **2**, triplicate sets of ten 0.5 mL low protein binding Eppendorf tubes were prepared. Working solutions of **2** (1% DMSO (w/v), 5 µL) in a range of ten concentrations (100, 50, 25, 12.5, 6.3, 3.1, 1.6, 0.8, 0.4, 0 µM) were prepared with MilliQ water and kept on ice. The reaction mixture was prepared by adding 35 µL of enzyme working solution (200 nM AcGH79, 20 mM HEPES, 150 mM NaCl, pH 7.4) with 210 µL of McIlvaine (pH 5.0, 150 mM) and with 35 µL of 3 M NaCl solution. The reaction mixture (8 µL) was aliquoted into ten low protein binding Eppendorf tubes in triplicate while on ice, and the inhibitor solutions (1 µL) were added into the respective tubes containing the reaction mixture. In a separate low protein binding Eppendorf tube, 1 µL of 10% (w/v) DMSO was added to the reaction mixture in place of the inhibitor solution. Tubes were pre-incubated at 37 °C for 60 min in a thermoshaker at 800 rpm. Next, 1 µL of ABP **7** working solution (1% (w/v) DMSO, 1 µM) was added to each tube, and the reactions were incubated at 37 °C for 30 min while shaking. Reactions were stopped by loading 2.5 µL of 5× Laemmli buffer (0.3 M Tris-HCl pH 6.8, 50 % (v/v) 100 % glycerol, 8 % (w/v) dithiothreitol (DTT), 10 % (w/v) sodium dodecyl sulfate (SDS), 0.01 % (w/v) bromophenol blue), followed by denaturation at 98 °C for 5 min. Electrophoresis in sodium dodecylsulfate (SDS-PAGE) and in-gel fluorescence detection were carried out according to previously described procedures. For quantification of the *in vitro* apparent IC₅₀ values, intensities of fluorescently labeled bands were calculated with 1D Image Quant Gel analysis software, and normalized to the corresponding band in the inhibitor-free control lane. Data were plotted and analysed in GraphPad Prism. The calculated IC₅₀ values from three independent sets measured for each inhibitor were used to calculate the average and the standard deviation (S.D.) of the *in vitro* apparent IC₅₀ value of each inhibitor.

HPSE – The *in vitro* apparent IC₅₀ values of **1-3** against recombinant HPSE were measured by in-gel competitive ABPP with ABP **7** (as described in Chapter 2) as fluorescent read-out. The enzymatic reactions were carried out at a constant concentration of enzyme (20 nM, final) and of read-out **7** (100

nM, final). For inhibitors, duplicate sets of six 0.5 mL low protein binding Eppendorf tubes were prepared. Working solutions of inhibitors (1% DMSO (w/v), 5 μ L) in a range of six concentrations (100, 20, 4, 0.8, 0.16, 0.03 μ M) were prepared with MilliQ water and kept on ice. The reaction mixture was prepared by adding 35 μ L of enzyme working solution (200 nM rhHPSE, 20 mM HEPES, 150 mM NaCl, pH 7.4) with 210 μ L of McIlvaine (pH 5.0, 150 mM) and with 35 μ L of 3 M NaCl solution. The reaction mixture (8 μ L) was aliquoted into ten low protein binding Eppendorf tubes in duplicate while on ice, and the inhibitor solutions (1 μ L) were added into the respective tubes containing the reaction mixture. In a separate low protein binding Eppendorf tube, 1 μ L of 10% (w/v) DMSO was added to the reaction mixture in place of the inhibitor solution. Tubes were pre-incubated at 37 °C for 60 min in a thermoshaker at 800 rpm. Next steps followed the same procedure used for AcGH79 as described in the section above (*Determination of in vitro apparent IC₅₀ values – AcGH79*).

Competitive ABPP experiments in platelet lysates

For competitive ABPP, the protein mixture was prepared by mixing the platelet lysates (87.5 μ L), buffer (pH 5.0, 150 mM, 157.5 μ L) and 3 M NaCl solution (35 μ L). The enzymatic reactions were carried out at a constant concentration of read-out **7** (100 nM, final). For each inhibitor **1-3**, triplicate sets of ten 0.5 mL low protein binding Eppendorf tubes were prepared. Working solutions of each inhibitor (1% DMSO (w/v), 5 μ L) in a range of ten concentrations (100, 50, 25, 12.5, 6.3, 3.1, 1.6, 0.8, 0.4, 0 μ M) were prepared with MilliQ water and kept on ice. The working protein mixture (8 μ L) was added in each protein low binding 0.5 mL Eppendorf tube, and 1 μ L of inhibitor solution was added while on ice. Next steps followed the procedure described above (*Determination of in vitro apparent IC₅₀ values – AcGH79*).

3.5.2 Chemical synthesis

General experimental details

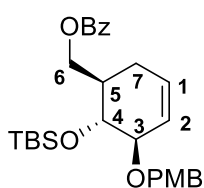
Chemicals were purchased from Acros, Sigma Aldrich, Biosolve, VWR, Fluka, Merck and Fisher Scientific and used as received unless stated otherwise. Tetrahydrofuran (THF), dichloromethane (DCM), *N,N*-dimethylformamide (DMF) and toluene were stored over molecular sieves before use. Traces of water from reagents were removed by co-evaporation with toluene in reactions that required anhydrous conditions. All reactions were performed under an argon atmosphere unless stated otherwise. TLC analysis was conducted using Merck aluminum sheets (Silica gel 60 F254) with detection by UV absorption (254 nm), by spraying with a solution of (NH₄)₆Mo₇O₂₄·4H₂O (25 g/L) and (NH₄)₄Ce(SO₄)₄·2H₂O (10 g/L) in 10% sulfuric acid or a solution of KMnO₄ (20 g/L) and K₂CO₃ (10 g/L) in water, followed by charring at ~150 °C. Column chromatography was performed using Screening Device b.v. silica gel (particle size of 40 – 63 μ m, pore diameter of 60 Å) with the indicated eluents. For reversed-phase HPLC purifications an Agilent Technologies 1200 series instrument equipped with a semi-preparative column (Gemini C18, 250 x 10 mm, 5 μ m particle size, Phenomenex) was used.

LC/MS analysis was performed on a Surveyor HPLC system (Thermo Finnigan) equipped with a C18 column (Gemini, 4.6 mm x 50 mm, 5 μ m particle size, Phenomenex), coupled to a LCQ Advantage Max (Thermo Finnigan) ion-trap spectrometer (ESI⁺). Reversed-phase HPLC purification was performed on an Agilent Technologies 1200 series instrument equipped with a HILIC column (VP 250/10 Nucleodur HILIC, 5 μ m particle size, Macherey-Nagel). The applied buffers were: (A) 1% AcOH in H₂O, and (B) CH₃CN. ¹H NMR and ¹³C NMR spectra were recorded on a Brüker AV-400 (400 and 101 MHz respectively) Brüker AV-500 (500 MHz and 126 MHz), Brüker DMX-600 (600 and 151 MHz), or a Brüker AV-850 (850 and 214 MHz) spectrometer in the given solvent. Chemical shifts (δ) are given in ppm relative to tetramethylsilane (TMS) as internal standard (0 ppm in ¹H NMR with CDCl₃) or the residual signal of the deuterated solvent. Coupling constants (*J*) are given in Hz. All given ¹³C-NMR spectra are proton decoupled. The following abbreviations are used to describe peak patterns when appropriate: s (singlet), d (doublet), t (triplet), q (quartet), m (multiplet), Ar (aromatic), C_q (quaternary carbon). 2D NMR experiments (COSY, HSQC) were carried out to assign protons and carbons of the new structures. High-resolution mass spectrometry (HRMS) analysis was performed with a LTQ Orbitrap mass spectrometer (Thermo Finnigan), equipped with an electrospray ion source in positive mode (source voltage 3.5 kV, sheath gas flow 10 mL/min, capillary temperature 250 °C) with resolution *R* = 60000 at *m/z* 400 (mass range *m/z* = 150 – 2000) and dioctyl phthalate (*m/z* = 391.28428) as a “lock mass”. The high-resolution mass spectrometer was calibrated prior to measurements with a calibration mixture (Thermo Finnigan).

Experimental Procedures and Characterisation Data of Products

The spectroscopic data of **7**³⁸, **9**³⁹ and **18**⁴³ are in agreement with those previously reported.

Compound 10

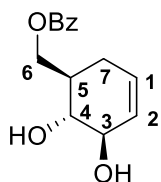


Alcohol **9** (1.9 g, 5 mmol) was dissolved in anhydrous DCM (25 mL), the solution was then degassed with N₂ and cooled to 0 °C (ice bath). BzCl (872 μ L, 7.5 mmol) and pyridine (604 μ L, 7.5 mmol) were then added and the mixture was allowed to attain room temperature while stirring. Full conversion was observed after 1 h and 30

minutes, after which the reaction mixture was diluted with DCM (125 mL), transferred to a separatory funnel and washed two times with a saturated aqueous solution of NaHCO₃ (2x 50 mL). The organic layer was dried over Na₂SO₄, filtered and concentrated under reduced pressure to obtain a colourless oil. Purification by silica gel column chromatography (pentane/EtOAc 99:1 \rightarrow 95:5) yielded the titled compound as a colourless oil (2.29 g, 4.75 mmol, 95% yield). ¹H NMR (400 MHz, CDCl₃): δ = 8.07 – 8.00 (m, 2H, 2CH Ar, 7.58 – 7.46 (m, 1H, 1CH Ar, Bz), 7.46 – 7.37 (m, 2H, 2CH Ar, Bz), 7.32 – 7.24 (m, 2H, 2CH Ar, PMB), 6.90 – 6.82 (m, 2H, 2CH Ar, PMB), 5.80 – 5.66 (m, 2H, H-1/ H-2), 4.62 – 4.48 (m, 3H, CHH-6/ CH₂PhOMe), 4.41 – 4.32 (m, 1H, CHH-6), 3.95 – 3.87 (m, 2H, H-3/ H-4), 3.77 (s, 3H, OMe, PMB), 2.33 – 2.20 (m, 1H, CHH-7), 2.24 – 2.10 (m, 2H, CHH-7/ H-5), 0.89 (s, 9H, C(CH₃)₃, TBS) ppm. ¹³C NMR (101 MHz, CDCl₃): δ = 166.5, 159.1 (2C_q), 132.9 (CH Ar, Bz), 130.7 (C_q, PMB), 130.3

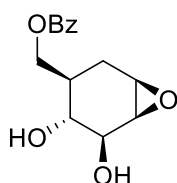
(C_q, PMB), 129.5 (2CH Ar, Bz), 129.3 (2CH Ar, PMB), 128.4 (2CH Ar, Bz), 127.8 (CH, C-2), 125.7 (CH, C-1), 113.7 (2CH Ar, PMB), 81.0 (CH, C-3), 72.3 (CH, C-4), 70.8 (CH₂, PMB), 65.4 (CH₂, C-6), 55.2 (OMe, PMB), 39.7 (CH, C-5), 27.9 (CH₂, C-7), 26.1 (C(CH₃)₃, TBS), 18.3 (C(CH₃)₃, TBS), -3.85, -4.9 (Si(CH₃)₂, TBS) ppm. HR-MS (ESI): *m/z* calcd for C₂₈H₃₈O₅SiNa⁺: 505.2381 [*M*+Na]⁺, found: 505.2378.

Compound 11



Alkene **10** (6.76 g, 14 mmol) was dissolved in THF (70 mL) followed by addition of a 1 M solution of TBAF in THF (112 mL, 112 mmol). The reaction was left stirring for 1 h at room temperature, after which final conversion could be observed by TLC. The reaction mixture was quenched by addition of a saturated NaHCO₃ aqueous solution (100 mL) and Et₂O (900 mL), and transferred to a separatory funnel. The aqueous layer was the extracted twice with Et₂O (200 mL) The combined organic layers were then dried over Na₂SO₄, filtered and concentrated under reduced pressure. The crude was taken up in DCM (280 mL) and a pH 7.4 aqueous phosphate buffer (120 mL) was added. The solution was cooled on ice and 2,3-dichloro-5,6-dicyano-1,4-benzoquinone (DDQ) (19 g, 84 mmol) was subsequently added. After stirring at room temperature in darkness for 1 hour, full conversion was observed. The reaction was quenched by the addition of a saturated aqueous solution of NaHCO₃ (130 mL) and Na₂S₂O₃ (130 mL), diluted with DCM (550 mL) and transferred to a separatory funnel. The two layers were then separated and the aqueous layer was extracted twice with DCM (500 mL). The combined organic layers were dried over Na₂SO₄, filtered and concentrated under reduced pressure. The crude was purified by silica gel chromatography (pentane/EtOAc 20:1→1:1) and the title compound was collected as a thick colourless oil (2.73 g, 11.0 mmol, 79% yield over two steps). ¹H NMR (400 MHz, CDCl₃): δ = 8.07 – 8.00 (m, 2H, 2CH Ar), 7.58 (ddt, *J* = 7.9, 7.0, 1.3 Hz, 1H, 1CH Ar), 7.49 – 7.40 (m, 2H, 2CH Ar), 5.75 – 5.66 (m, 1H, H-1), 5.64 – 5.55 (m, 1H, H-2), 4.84 (dd, *J* = 11.4, 4.2 Hz, 1H, CHH-6), 4.32 – 4.18 (m, 2H, H-3/CHH-6), 3.64 (s, 1H, 3-OH), 3.47 (dd, *J* = 11.1, 7.8 Hz, 1H, H-4), 2.70 (s, 1H, 4-OH), 2.34 – 2.18 (m, 2H, H-7), 2.18 – 2.02 (m, 1H, H-5) ppm. ¹³C NMR (101 MHz, CDCl₃): δ = 167.6 (C_q, C=O, Bz), 133.6, 129.9, 128.6 (5CH Ar, Bz), 128.5 (CH, C-2), 127.5 (CH, C-1), 73.7 (CH, C-4), 73.5 (CH, C-3), 64.9 (CH₂, C-6), 39.6 (CH, C-5), 28.7 (CH₂, C-7) ppm. HR-MS (ESI): *m/z* calcd for C₁₄H₁₆O₄Na⁺: 271.0941 [*M*+Na]⁺, found: 271.0938.

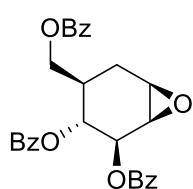
Compound 12



Compound **11** (0.51 g, 2.1 mmol) was dissolved in anhydrous DCM (20 mL) and the solution was cooled to -5 °C (ice/salt bath). *m*-CPBA (<77% wt, 0.93 g, 4.1 mmol) was added at -5 °C, and the reaction mixture was stirred overnight while allowed to reach 4 °C. Upon full conversion the reaction was quenched by the addition of a saturated aqueous solution of Na₂S₂O₃ (50 mL), diluted with DCM (250 mL) and transferred to a

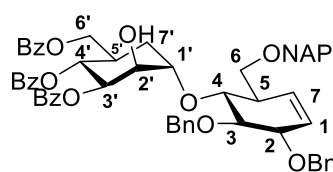
separatory funnel. The two layers were separated and the organic solution was washed twice with a saturated aqueous solution of NaHCO_3 (50 mL) and brine solution. The organic layer was then dried using Na_2SO_4 , filtered and concentrated under reduced pressure. The crude was purified by silica gel chromatography (pentane/EtOAc 2:3 \rightarrow 1:4) to yield the title compound as a pale yellow oil (0.37 g, 1.4 mmol, 67% yield). ^1H NMR (400 MHz, CDCl_3): δ = 8.10 – 7.99 (m, 2H, 2CH Ar), 7.63 – 7.54 (m, 1H, 1CH Ar), 7.50 – 7.35 (m, 2H, 2CH Ar), 4.72 (dd, J = 11.5, 4.0 Hz, 1H, CHH-6), 4.17 (dd, J = 11.4, 3.0 Hz, 1H, CHH-6), 3.91 (dd, J = 8.3, 1.9 Hz, 1H, H-3), 3.54 – 3.46 (m, 1H, H-4), 3.40 (ddd, J = 4.0, 1.8, 0.7 Hz, 1H, H-2), 3.32 (t, J = 4.3 Hz, 1H, H-1), 2.23 – 2.02 (m, 2H, H-7), 1.88 (m, J = 11.3, 7.0, 4.2, 2.9 Hz, 1H, H-5) ppm. ^{13}C NMR (101 MHz, CDCl_3): δ = 167.7 (C_q , C=O, Bz), 134.0, 129.9, 128.6 (5CH Ar, Bz), 74.1 (CH, C-3), 70.2 (CH, C-4), 64.0 (CH_2 , C-6), 56.5 (C-2), 53.1 (CH, C-1), 39.8 (CH, C-5), 26.3 (CH_2 , C-7) ppm. HR-MS (ESI): m/z calcd for $\text{C}_{14}\text{H}_{16}\text{O}_5\text{Na}^+$: 287.09408 [$M+\text{Na}$] $^+$, found: 287.09397.

Compound 8



Epoxide **12** (832.2 mg, 0.315 mmol) was dissolved in dry pyridine (1.65 mL, 0.191 M) and cooled to 0 °C (ice bath). BzCl (99 wt%, 123.2 μL , 1.05 mmol, 3.5 eq.) was then added dropwise. The stirring continued at 0 °C for 2 h and 30 minutes, when full conversion could be observed. The reaction was then quenched by the addition of a saturated aqueous solution of NaHCO_3 , while at 0 °C. The mixture was transferred to a separatory funnel, extracted two times with EtOAc (50 mL), then washed twice, first with H_2O (20 mL) then with brine solution (20 mL). The organic layers were then collected, dried over Na_2SO_4 , filtered, and concentrated under reduced pressure. The crude was then purified by silica gel chromatography (pentane/EtOAc 9:1 \rightarrow 2:3), affording the title compound as a dense milky oil (128.6 mg, 0.27 mmol, 84% yield). ^1H NMR (400 MHz, CDCl_3): δ = 8.09 - 7.47 (m, 6H, 6CH Ar), 7.57 – 7.27 (m, 10H, 10CH Ar), 5.78 (dd, J = 11.0, 8.9 Hz, 1H, H-4), 5.65 (dd, J = 8.9, 1.9 Hz, 1H, H-3), 4.39 (dd, J = 11.3, 4.0 Hz, 1H, CHH-6), 4.24 (dd, J = 11.3, 5.2 Hz, 1H, CHH-6), 3.66 (dd, J = 3.8, 2.1 Hz, 1H, H-2), 3.45 (t, J = 4.3 Hz, 1H, H-1), 2.54 – 2.35 (m, 2H, H-5/CHH-7), 2.26 – 2.13 (m, 1H, CHH-7) ppm. ^{13}C NMR (101 MHz, CDCl_3): δ = 166.5, 166.0 (3 C_q , 3C=O, Bz), 133.4, 133.3, 133.2, 130.1, 129.8, 128.5, 128.4 (15CH Ar, Bz), 74.4 (CH, C-3), 70.2 (CH, C-4), 64.1 (CH_2 , C-6), 54.9 (CH, C-2), 52.9 (CH, C-1), 38.0 (CH, C-5), 26.6 (CH_2 , C-7) ppm. HR-MS (ESI): m/z calcd for $\text{C}_{28}\text{H}_{25}\text{O}_7^+$: 473.15948 [$M+\text{H}$] $^+$, found 473.15910.

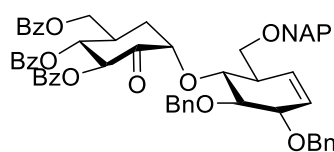
Compound 5



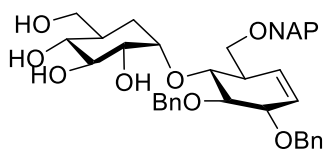
Epoxide **7** (2.28 g, 4.83 mmol) and cyclohexene **6** (9.29 g, 19.3 mmol) were combined in a flask, co-evaporated thrice with dry distilled toluene and dissolved in dry DCM (19.3 mL). The mixture was cooled to 0 °C, and $\text{BF}_3\cdot\text{OEt}_2$ (298 μL , 2.42 mmol) was added. The reaction was stirred for 16 h whilst allowing the cooling bath to slowly warm to room temperature. Next, the reaction was cooled to 0 °C and quenched with Et_3N (506 μL , 3.62 mmol). The mixture was diluted with sat. aq.

NaHCO₃ (50 mL) and extracted with DCM (3 x 250 mL). The combined organic layers were dried over MgSO₄, filtered and concentrated. Flash purification by silica column chromatography (pentane:Et₂O, 10:1→1.5:1) with wet load (distilled toluene) afforded first the cyclohexene starting material **6** as white solid (5.85 g) and then desired product **5** as an oil (3.45 g, 3.62 mmol, 75 % yield). ¹H NMR (400 MHz, CDCl₃): δ = 7.98 – 7.66 (m, 11H, 11CH Ar/toluene traces), 7.51 – 7.08 (m, 26H, 21CH Ar/toluene traces/CDCl₃), 5.81 – 5.68 (m, 3H, H-7, H-1, H-4'), 5.54 (dd, *J* = 9.4, 2.9 Hz, 1H, H-3'), 5.14 (d, *J* = 11.4 Hz, 1H, 1CH Ar), 4.83 – 4.74 (d, *J* = 11.4 Hz, 1H, 1CH Ar), 4.74 – 4.56 (m, 4H, 4CH Ar), 4.29 (ddd, *J* = 5.3, 3.3, 1.6 Hz, 1H, H-2), 4.24 (dd, *J* = 11.3, 4.8 Hz, 2H, CHHOBz, H-9), 4.19 – 4.14 (m, 2H, H-2', CHHOBz), 4.13 – 4.06 (m, 1H, H-1'), 3.83 (dd, *J* = 9.9, 7.5 Hz, 1H, H-3), 3.73 (t, *J* = 9.5 Hz, 1H, H-4), 3.66 (d, *J* = 4.0 Hz, 2H, CH₂ONAP), 2.64 – 2.55 (m, 1H, H-5), 2.55 – 2.46 (m, 1H, H-5') 1.92 – 1.71 (m, 2H, CH₂, H-7') ppm. ¹³C NMR (101 MHz, CDCl₃): δ = 166.4, 166.0, 165.8, 139.0, 138.3, 135.6, 133.2 (7C_q), 133.1, 133.0, 132.9, 130.0, 129.8, 129.7, 129.5, 128.5, 128.4, 128.3, 128.0, 127.9, 127.8, 127.7, 127.6, 127.5, 126.6, 126.5, 126.3, 126.2, 126.0, 125.7 (32CH Ar), 85.0 (CH, C-3), 81.5 (CH, C-2), 78.2 (CH, C-1'), 77.9 (CH, C-4), 75.2 (CH₂Ph), 74.5 (CH, C-3'), 73.3 (CH₂Ph), 71.5 (CH₂Ph), 71.0 (CH, C-2'), 70.8 (CH, C-4'), 69.6 (CH₂, C-6'), 65.0 (CH₂, C-6), 44.2 (CH, C-5), 36.2 (CH, C-5'), 27.1 (CH₂, C-7') ppm. HR-MS (ESI): *m/z* calcd for C₆₀H₅₆O₁₁Na⁺: 975.37148 [*M*+Na]⁺, found 975.37129.

Compound 13

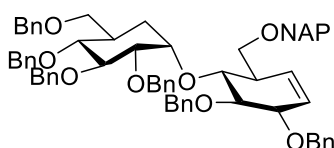


Axial alcohol **5** (0.84 g, 0.88 mmol) was coevaporated with dry distilled toluene, and dissolved in dry DCM (13 mL). At 0 °C, DMP (0.74 g, 1.8 mmol) was added portion-wise. The reaction mixture was allowed to gradually attain rt overnight. After 17 h, celite was added, and the solution was concentrated to dryness. Crude was purified by silica column chromatography with dry-load (pentane/Et₂O 10:1→1.5:1), affording the desired product as off-white solid (0.72 g, 0.76 mmol, 86% yield). ¹H NMR (400 MHz, CDCl₃): δ = 8.05 – 7.61 (m, 11H, 11CH Ar, Bz/NAP), 7.61 – 6.88 (m, 25H, 21CH Ar/CDCl₃), 6.28 (dd, *J* = 10.2, 1.2 Hz, 1H, H-3'), 5.79 (dt, *J* = 10.3, 2.2 Hz, 1H, H-1), 5.69 (dt, *J* = 10.0, 2.1 Hz, 1H, H-7), 5.63 (t, *J* = 10.4 Hz, 1H, H-4'), 4.89 (dd, *J* = 21.1, 9.9 Hz, 2H, CH₂Ph), 4.76 – 4.52 (m, 4H, 2CH₂Ph), 4.38 (t, *J* = 3.0 Hz, 1H, H-1'), 4.26 (q, *J* = 2.8 Hz, 1H, H-2), 4.17 (ddd, *J* = 26.3, 15.0, 3.8 Hz, 2H, CH₂-6'), 3.95 – 3.82 (m, 2H, H-3, H-4), 3.66 (ddd, *J* = 13.6, 9.3, 3.3 Hz, 2H, CH₂, H-6), 2.96 – 2.84 (m, 1H, H-5'), 2.70 – 2.61 (m, 1H, H-5), 1.99 (dt, *J* = 15.0, 3.6 Hz, 1H, CHH-7'), 1.52 – 1.43 (m, 1H, CHH-7') ppm. ¹³C NMR (101 MHz, CDCl₃): δ = 199.1 (C=O, C-2'), 166.2, 165.3, 138.9, 138.3, 135.4 (5C_q), 133.4, 133.3 (2CH Ar), 133.2 (C_q), 133.2 (CH Ar), 133.1 (C_q), 130.1, 130.0, 129.9, 129.7 (4CH Ar), 129.2, 129.1 (2C_q), 129.0, 128.6, 128.5, 128.4, 128.3, 128.2, 128.0, 127.9, 127.7, 127.3, 126.9, 126.8, 126.4, 126.1, 125.9 (25CH Ar), 82.8 (CH, C-3), 81.2 (CH, C-1'), 80.8 (CH, C-2), 77.7 (CH, C-4), 77.6 (CH, C-3'), 74.0 (CH₂Ph), 73.4 (CH₂Ph), 72.8 (CH, C-4'), 71.6 (CH₂Ph), 69.6 (CH₂, C-6), 63.6 (CH₂, C-6'), 43.8 (CH, C-5), 35.2 (CH, C-5'), 30.4 (CH₂, C-7') ppm. HR-MS (ESI): *m/z* calcd for C₆₀H₅₅O₁₁⁺ 951.37389 [*M*+H]⁺, found 951.37383.

Compound 14

Ketone **13** (0.39 g, 0.41 mmol) was coevaporated thrice with dry distilled toluene, dissolved in dry THF/MeOH (1:1 v/v, 4 mL) and the resulting solution was cooled to $-60\text{ }^{\circ}\text{C}$. At $-60\text{ }^{\circ}\text{C}$, NaBH_4 (54 mg, 1.4 mmol) was added portion-wise. The reaction mixture was allowed to progressively

warm up to $0\text{ }^{\circ}\text{C}$ over 4 h, and stirred at this temperature overnight. The reaction was quenched by addition of acetone, then Celite was added and the mixture was concentrated to dryness. The crude was dry-loaded on a silica gel column and flash purification (pentane/EtOAc, 7:1 \rightarrow 1:4) afforded the title equatorial product **12** (0.24 mg, 0.38 mmol, 92%) as a pale yellow oil. ^1H NMR (600 MHz, CDCl_3): $\delta = 7.87 - 7.77$ (m, 4H, 4CH Ar), $7.52 - 7.25$ (m, 16H, 13CH Ar/ CDCl_3), 5.79 (dt, $J = 10.6, 2.6$ Hz, 1H, H-7), 5.68 (dt, $J = 10.2, 2.0$ Hz, 1H, H-1), 5.12 (d, $J = 10.8$ Hz, 1H, 1CHHPh), $4.74 - 4.69$ (m, 2H, CH_2Ph), $4.65 - 4.58$ (m, 3H, 3CHHPh), $4.34 - 4.27$ (m, 1H, H-2), $3.91 - 3.83$ (m, 1H, H-4), 3.75 (dd, $J = 9.9, 7.1$ Hz, 1H, H-3), $3.56 - 3.51$ (m, 2H, CH_2 , H-6), $3.49 - 3.45$ (m, 1H, H-1'), $3.42 - 3.36$ (m, 2H, CH_2 , H-6'), 3.25 (t, $J = 9.4$ Hz, 1H, H-3'), 3.09 (t, $J = 9.9$ Hz, 1H, H-4'), $2.85 - 2.76$ (m, 1H, H-2'), $2.46 - 2.40$ (m, 1H, H-5), $1.91 - 1.82$ (m, 1H, H-5'), 1.30 (dt, $J = 13.9, 3.3$ Hz, 1H, $\frac{1}{2}$ CH_2 , CHH-7'), 0.51 (td, $J = 13.9, 2.1$ Hz, 1H, CHH-7') ppm. ^{13}C NMR (151 MHz, CDCl_3): $\delta = 138.0, 137.5, 135.2, 133.3, 133.2$ (5 C_q), 129.7 (CHsp^2 , C-1), $128.8, 128.7, 128.6, 128.4, 128.3, 128.2, 128.0, 127.9, 127.8, 127.4, 126.4, 126.3$ (17CH Ar), 126.1 (CHsp^2 , C-7), 126.0 (CH Ar), 83.5 (CH, C-3), 80.8 (CH, C-2), 79.5 (CH, C-1'), 79.0 (CH, C-4), 76.8 (CH, C-4'), 75.9 (CH, C-2'/C-3'), 75.6 (CH, C-2'/C-3'), $75.5, 73.6, 71.6$ (3 CH_2Ph), 69.0 (CH_2 , C-6), 66.8 (CH_2 , C-6'), 45.8 (CH, C-5), 37.9 (CH, C-5'), 29.9 (CH_2 , C-7') ppm. HR-MS (ESI): m/z calcd for $\text{C}_{39}\text{H}_{45}\text{O}_8^+$: 641.31089 [$M+\text{H}$] $^+$, found 641.31067.

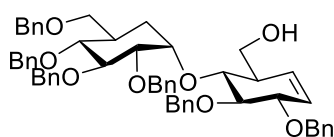
Compound 15

Alkene **14** (0.37 g, 0.57 mmol) was dissolved in dry DMF (2.9 ml, 0.2 M) and cooled to $0\text{ }^{\circ}\text{C}$. At $0\text{ }^{\circ}\text{C}$, NaH (60% wt, 0.18 g, 4.6 mmol) was added portion-wise and the solution was stirred for 15 minutes. BnBr

(0.57 ml, 4.5 mmol) was added, and the solution was allowed to slowly warm up to room temperature. After 18 h, reaction showed complete conversion. The reaction mixture was quenched at $0\text{ }^{\circ}\text{C}$ with water, diluted with Et_2O (20 ml) and washed with brine (2x 5 ml). The organic layers were dried over Na_2SO_4 , filtered, and concentrated to dryness. The crude was wet-loaded onto a silica gel column as concentrated solution in distilled toluene, and purified by silica gel column chromatography (pentane: Et_2O 50:1 \rightarrow 1:1), affording the titled compound as a pale yellow oil (0.42 g, 0.42 mmol, 73%). ^1H NMR (500 MHz, CDCl_3): $\delta = 7.84 - 7.64$ (m, 4H, 4CH Ar), $7.49 - 7.11$ (m, 36H, 28CH Ar/toluene traces/ CDCl_3), 5.77 (dt, $J = 10.2, 2.3$ Hz, 1H, H-7), 5.67 (dt, $J = 10.0, 2.1$ Hz, 1H, H-1), $5.08 - 4.79$ (m, 4H, 2 CH_2Ph), $4.75 - 4.52$ (m, 10H, 5 CH_2Ph), $4.26 - 4.22$ (m, 2H, H-2/H-1'), 4.03 (t, $J = 8.6$ Hz, 1H, H-4), 3.98 (t, $J = 9.3$ Hz, 1H, H-3'), 3.89 (dd, $J = 9.1, 6.9$ Hz, 1H, H-3), 3.72 (dd, $J = 9.0, 4.3$ Hz, 1H, $\frac{1}{2}$ CH_2), $3.68 - 3.60$ (m, 1H), 3.54 (ddd, $J = 11.0, 9.0, 3.7$ Hz, 2H, CH_2), 3.46 (dd, $J = 10.8, 8.9$ Hz, 1H, H-4'), 3.30 (dd, $J =$

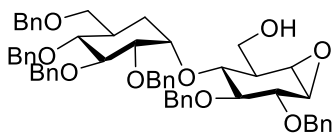
9.8, 2.9 Hz, 1H, H-2'), 3.19 (dd, $J = 9.0, 2.5$ Hz, 1H), 2.68 – 2.60 (m, 1H, H-5), 2.09 (dd, $J = 14.7, 3.9$ Hz, 1H, CHH-7'), 2.03 (t, $J = 11.8$ Hz, 1H, H-5'), 1.36 – 1.31 (m, 1H, CHH-7') ppm. ^{13}C NMR (101 MHz, CDCl_3): $\delta = 139.4, 138.7, 138.6, 138.5, 135.9, 133.3, 133.0$ (7C_q), 130.0 (CHsp^2 , C-1), 128.5, 128.4, 128.3, 128.2, 128.0, 127.9, 127.8, 127.7, 127.6, 127.5, 127.4, 127.2, 127.0 (18CH Ar), 126.6 (CHsp^2 , C-7), 126.2, 125.9, 125.7 (4CH Ar), 84.8 (CH, C-3), 83.8 (CH, C-3'), 83.0 (CH, C-2'), 81.0, 80.8 (2CH, C-2, C-4'), 75.4, 75.2 (2 CH_2Ph), 73.2 (CH, C-1'), 73.0 (CH_2Ph), 72.4 (CH, C-4), 72.4, 71.6, 70.0, 69.9 (4 CH_2Ph), 44.1 (CH, C-5) 37.1 (CH, C-5'), 27.9 (CH_2 , C-7') ppm. HR-MS (ESI): m/z calcd for $\text{C}_{67}\text{H}_{69}\text{O}_8^+$: 1001.49870 [$M+\text{H}$] $^+$, found 1001.49801.

Compound 16



Alkene **15** (0.42 g, 0.42 mmol) was dissolved in a mixture of DCM/ H_2O (10:1 v/v, 8.4 mL) and stirred vigorously in darkness. DDQ (0.11 g, 0.47 mmol) was added at rt. After 90 minutes, reaction showed complete conversion. The reaction mixture was quenched with saturated NaHCO_3 aqueous solution (1 mL), and diluted with DCM (60 mL). The solution was washed with saturated NaHCO_3 aqueous solution (4 x 15 mL), then brine (15 mL). The organic layer was dried over Na_2SO_4 , filtered, and concentrated to dryness. Purification by silica gel column chromatography (pentane/ Et_2O 50:1 \rightarrow 1:4), yielded the titled product as an oil (0.21 g, 0.24 mmol, 58% yield). ^1H NMR (500 MHz, CDCl_3): $\delta = 7.40 - 7.08$ (m, 37H, H-1', 30CH Ar, CDCl_3), 5.81 (dt, $J = 10.2, 2.5$ Hz, 1H, H-1), 5.65 (dt, $J = 10.1, 2.2$ Hz, 1H, H-7), 5.05 – 4.80 (m, 4H), 4.73 (d, $J = 10.9$ Hz, 1H), 4.48 – 4.40 (m, 3H,), 4.25 – 4.18 (m, 1H, H-2), 4.04 – 3.89 (m, 4H, CHH-6, H-4, H-3, H-3'), 3.64 (dd, $J = 11.0, 3.0$ Hz, 1H, CHH-6), 3.55 (dd, $J = 8.5, 2.7$ Hz, 1H, CHH-6'), 3.37 – 3.18 (m, 3H, H-2', H-4', CHH-6'), 2.73 (s, 1H, OH), 2.57 – 2.49 (m, 1H, H-5), 2.35 (dt, $J = 14.8, 3.3$ Hz, 1H, CHH-7'), 2.16 – 2.05 (m, 1H, H-5'), 1.13 (t, $J = 13.1$ Hz, 1H, CHH-7') ppm. ^{13}C NMR (126 MHz, CDCl_3): $\delta = 139.4, 139.2, 138.7, 138.6, 138.4, 138.1$ (6C_q), 129.9, 128.5, 128.4, 128.3, 128.2, 128.0, 127.9, 127.8, 127.7, 127.6, 127.5, 127.4, 127.1, 126.8, 125.6 (30CH Ar), 84.1, 84.0 (2CH, C-4, C-3), 82.6 (CH, C-2'), 81.4, 80.7 (2CH, C-2, C-4'), 75.6, 75.3 (2 CH_2Ph), 73.5 (CH, C-1'), 73.4, 73.3 (2 CH_2Ph), 72.6 (CH-3' and CH_2Ph), 71.4 (CH_2Ph), 70.2 (CH_2 , C-6'), 62.2 (CH_2 , C-6), 45.2 (CH, C-5), 37.7 (CH, C-5'), 30.4 (CH/ CH_3 , grease), 28.3 (2 CH_2 , C-7') ppm. HR-MS (ESI): m/z calcd for $\text{C}_{56}\text{H}_{61}\text{O}_8^+$: 861.43610 [$M+\text{H}$] $^+$, found 861.43622.

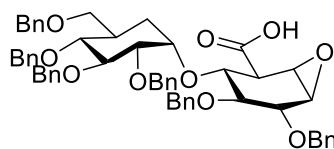
Compound 17



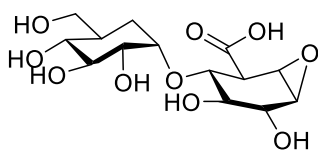
To a solution of alkene **16** (208 mg, 0.24 mmol) in dry DCM (2.7 mL) at -20 $^\circ\text{C}$, *m*-CPBA (<75%, 664 mg, 1.88 mmol) was added portion-wise. The solution was allowed to warm up to 4 $^\circ\text{C}$, and it was stirred for 18 hours at this temperature. Next, the solution was quenched with aqueous saturated NaHCO_3 solution and diluted with DCM. The organic layer was washed with further aqueous saturated NaHCO_3 solution, water and then brine. The combined organic layers were dried over Na_2SO_4 , filtered and concentrated.

Silica gel column chromatography of crude (P/Et₂O 50:1→1:4) afforded titled product (98 mg, 46%) as pale yellow oil and impure α -epoxide (10 mg, 5%). ¹H NMR (500 MHz, CDCl₃): δ = 7.59 – 6.87 (m, 30H, 30CH Ar), 4.98 – 4.34 (m, 13H, 6CH₂Ph, H-1'), 4.03 (dd, J = 11.0, 4.8 Hz, 1H, CHH-6), 3.97 – 3.92 (m, 1H, CHH-6), 3.92 – 3.55 (m, 4H), 3.52 – 3.40 (m, 1H, CHH-6'), 3.39 – 3.35 (m, 1H, H-7), 3.36 – 3.25 (m, 2H, CHH-6', CH), 3.15 (d, J = 3.9 Hz, 1H, H-1), 2.29 – 2.17 (m, 2H, H-5, CHH-7'), 2.14 – 1.97 (m, 1H, H-5'), 1.23 – 1.15 (m, 3H, CHH-7', grease) ppm. ¹³C NMR (101 MHz, CDCl₃): δ = 139.2, 138.8, 138.7, 138.4, 137.6 (6C_q), 133.8, 130.4, 129.9, 128.6, 128.5, 128.4, 128.3, 128.2, 128.1, 128.0, 127.9, 127.8, 127.7, 127.6, 127.4, 127.2, 126.6, 126.5 (30CH Ar), 85.0, 83.8, 82.5, 81.2, 80.2 (5CH), 75.4, 75.3 (2CH₂Ph), 73.5 (CH), 73.2, 72.7 (4CH₂Ph), 70.1 (CH₂, C-6'), 69.3 (CH), 62.2 (CH₂, C-6), 56.1 (CH, C-7, epoxide), 52.2 (CH, C-1, epoxide), 42.8 (CH, C-5), 37.6 (CH, C-5'), 27.8 (CH₂, C-7') ppm. HR-MS (ESI): m/z calcd for C₅₆H₆₁O₉⁺: 877.43101 [$M+H$]⁺, found 877.43007.

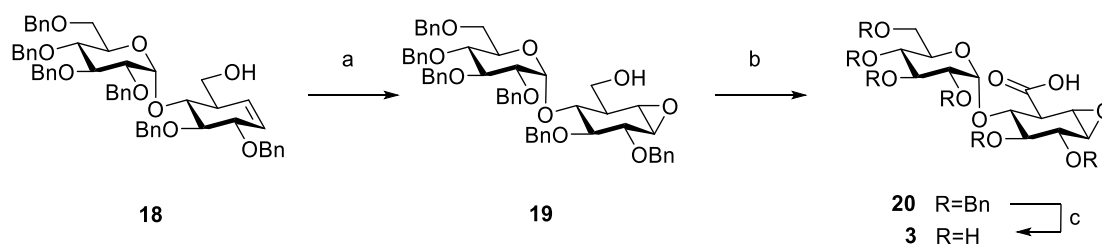
Compound 4



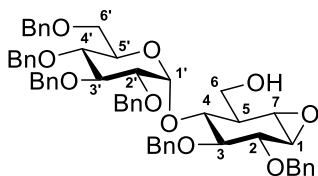
Epoxide **17** (83.3 mg, 0.0950 mmol) was co-evaporated twice with dry distilled toluene, and dissolved in DCM/^tBuOH/H₂O (4:5:1 v/v/v, 650 μ L). The solution was cooled to 0 °C. TEMPO (2.96 mg, 0.0185 mmol) and BAIB (78.1 mg, 0.238 mmol) were added at 0 °C. The solution was kept at this temperature during the reaction. After 3 h, TLC showed full consumption of the starting material, and the reaction was quenched with a saturated aqueous Na₂S₂O₃ solution (1 mL), diluted with H₂O (5 mL) and washed with DCM (40 mL). The collected aqueous layer was washed thrice with DCM (40 mL). Combined organic layers were dried over Na₂SO₄, filtered, and volatiles were removed. Crude was purified by flash chromatography over silica gel (pentane/EtOAc 20:1→3:2 +0.5% AcOH), affording the desired product as a pale yellow oil (60.2 mg, 71% yield). ¹H NMR (400 MHz, CDCl₃): δ = 7.44 – 6.88 (m, 30H, 30CH Ar), 4.95 – 4.28 (m, 13H, 6CH₂Ph, H-1'), 4.04 (t, J = 9.3 Hz, 1H, H-4), 3.98 – 3.82 (m, 2H, H-2/H-2'), 3.65 (dd, J = 9.1, 6.9 Hz, 1H, H-3), 3.48 (ddd, J = 23.0, 8.8, 3.6 Hz, 2H, CH₂-6'), 3.39 – 3.30 (m, 2H, H-7/H-4'), 3.26 (dd, J = 10.0, 3.2 Hz, 1H, H-3'), 3.16 (d, J = 3.8 Hz, 1H, H-1), 3.11 (dd, J = 9.5, 1.8 Hz, 1H, H-5), 2.17 (dt, J = 14.9, 3.8 Hz, 1H, CHH-7'), 2.05 – 1.90 (m, 1H, H-5'), 1.31 – 1.18 (m, 1H, CHH-7'). ¹³C NMR (101 MHz, CDCl₃): δ = 173.6 (C_q, C-6), 139.2, 139.0, 138.7, 138.4, 137.4 (5 C_q), 128.6, 128.6, 128.5, 128.4, 128.3, 128.2, 128.1, 128.0, 127.9, 127.8, 127.7, 127.5, 127.4, 127.3, 127.2, 126.8, 126.7 (17 CH Ar), 83.7, 83.5 (CH, C-2/C-2'), 82.5 (CH, C-3'), 81.3 (CH, C-4'), 81.1, 79.6 (CH, C-2/C-2'), 75.5, 75.2 (2CH₂Ph), 74.3 (CH, C-1'), 73.4, 73.3, 72.9, 72.7 (4CH₂Ph), 71.6 (CH, C-4), 70.3 (CH₂, C-6'), 53.9 (CH, C-7, epoxide), 52.9 (CH, C-1, epoxide), 48.3 (CH, C-5), 36.8 (CH, C-5'), 29.8 (CH₂, C-7') ppm. HR-MS (ESI): m/z calcd for C₅₆H₅₉O₁₀⁺: 891.41027 [$M+H$]⁺, found 891.40978.

Compound 2 (VB-B03-104)


Acid **4** (59 mg, 67 μmol) was dissolved in a mixture of MeOH/^tBuOH/dioxane (2:1:2 v/v/v, 6.7 mL) under Nitrogen, then Pd(OH)₂/C (20% wt, 61 mg, 87 μmol) was added. Under vigorous stirring, the mixture was flushed with a H₂ balloon. After stirring for 5 h under H₂ atmosphere, the mixture was filtered over a Whatman pad, concentrated, and purified by reverse-phase HPLC chromatography with HILIC column (gradient: 70-65% eluent B for 9 minutes, then 65-50% eluent B for 9 minutes). After lyophilisation, the desired product (7.3 mg, 21 μmol , 31%) was obtained as white powder. ¹H NMR (400 MHz, D₂O): δ = 3.91 – 3.82 (m, 1H, H-1'), 3.71 (d, *J* = 8.4 Hz, 1H, H-2), 3.58 (dd, *J* = 11.4, 4.8 Hz, 1H, CHH-6'), 3.50 (dd, *J* = 11.4, 3.3 Hz, 1H, CHH-6'), 3.47 – 3.25 (m, 5H, H-2', H-3, H-3', H-4, H-7), 3.11 (dd, *J* = 10.8, 9.1 Hz, 1H, H-4'), 3.03 (d, *J* = 3.7 Hz, 1H, H-1), 2.67 (dd, *J* = 9.6, 1.7 Hz, 1H, H-5), 1.79 (dt, *J* = 14.5, 3.7 Hz, 1H, CHH-7'), 1.71 – 1.60 (m, 1H, H-5'), 1.14 (td, *J* = 14.1, 1.7 Hz, 1H, CHH-7') ppm. ¹³C NMR (101 MHz, D₂O): δ = 178.0 (C_q, C-6), 80.2 (CH, C-1'), 78.2, 76.5, 75.1 (3 CH, C-3, C-4, C-3'), 74.2 (CH, C-2'), 72.8 (CH, C-4'), 70.9 (CH, C-2), 62.0 (CH₂, C-6'), 56.2 (CH, C-7, epoxide), 55.3 (CH, C-1, epoxide), 51.6 (CH, C-5), 38.2 (CH, C-5'), 28.8 (CH₂, C-7') ppm. HR-MS (ESI): *m/z* calcd for C₁₄H₂₃O₁₀⁺: 351.12857 [*M*+H]⁺, found 351.12845.



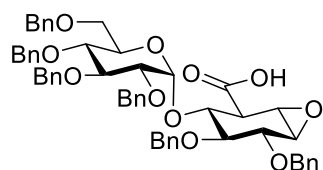
Scheme 3.S1. Reagents and conditions: a) Boc₂O, DMAP, THF; NIS, AcOH; then NaOMe, DCM/MeOH, 67% over 3 steps; b) TEMPO, BAIB, DCM/^tBuOH/H₂O, 82%; c) Na(s), ^tBuOH, NH₃, -60 °C, 80%.

Compound 19


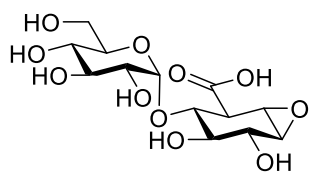
Compound **18** (0.12 g, 0.13 mmol) was co-evaporated thrice with anhydrous toluene and subsequently dissolved in 0.9 mL anhydrous THF. Boc₂O (0.062 mL, 0.26 mmol) and DMAP (0.013 g, 0.11 mmol) were added and the reaction was stirred overnight. The reaction mixture was quenched and diluted with H₂O. The water layer was extracted thrice with Et₂O, the combined organic layers were washed with sat. NH₄Cl (aq), sat. NaHCO₃ (aq), brine, dried over MgSO₄, filtered and concentrated *in vacuo*. The crude product was used without purification in the next step. Crude (0.13 mmol) was dissolved in 0.65 mL AcOH. NIS (0.058 g, 0.26 mmol) was added and the reaction was stirred overnight. The reaction mixture was diluted with Et₂O, quenched with Et₃N, washed with sat.

NaHCO₃ (aq), 10% Na₂S₂O₃, brine, dried over MgSO₄, filtered and concentrated *in vacuo*. The crude product was used without further purification in the next step. Crude was next dissolved in 0.65 mL MeOH/DCM (1/1, v/v, 0.65 mL) and NaOMe (5.4M in MeOH) was added catalytically. The reaction was stirred overnight. The reaction mixture was diluted with EtOAc, washed with H₂O, brine, dried over MgSO₄, filtered and concentrated *in vacuo*. The crude product was purified using flash silica column chromatography (pentane/EtOAc, 10:1→5:1) to obtain compound **20** (0.077 g, 0.088 mmol, 67% over 3 steps). ¹H NMR (400 MHz, CDCl₃): δ = 7.38 – 7.02 (m, 30CH, 30H Ar), 5.69 (d, *J* = 3.9 Hz, 1H, H-1'), 4.88 (t, *J* = 11.4 Hz, 2H, 2CHHPH), 4.82 – 4.65 (m, 4H, 4CHHPH), 4.60 – 4.39 (m, 6H, 6CHHPH), 4.03 – 3.85 (m, 6H), 3.73 – 3.64 (m, 2H), 3.63 – 3.57 (m, 1H), 3.52 – 3.45 (m, 2H, H-2', CH), 3.41 – 3.34 (m, 1H, H-1/H-7, epoxide), 3.15 (d, *J* = 3.8 Hz, 1H, H-1/H-7, epoxide), 2.60 – 2.52 (m, 1H, OH), 2.28 – 2.19 (m, 1H) ppm. ¹³C NMR (101 MHz, CDCl₃): δ = 139.1, 138.7, 138.1, 137.6, 137.5 (5C_q), 129.1, 128.6, 128.5, 128.4, 128.4, 128.3, 128.3, 128.2, 128.1, 128.0, 127.9, 127.8, 127.6, 127.5, 127.1, 126.4, 125.4 (19CH Ar), 97.3 (CH, C-1'), 84.8, 81.9, 80.1, 79.2, 78.0 (5CH), 75.5, 75.1, 73.7, 73.6, 73.1, 72.8 (6CH₂), 71.4, 70.0 (2CH), 68.7, 61.8 (2CH₂), 56.5 (CH, C-1/C-7), 52.4 (CH, C-1/C-7), 43.2 (CH, C-5) ppm. HR-MS (ESI): *m/z* calcd for C₅₅H₆₂O₁₀N⁺: 896.4368 [*M*+NH₄]⁺, found 896.4368.

Compound 20



Compound **19** (0.07 g, 0.08 mmol) was dissolved in DCM/^tBuOH/H₂O (4:4:1, v/v/v, 2.65 mL) and cooled down to 0 °C. TEMPO (0.0025 g, 0.016 mmol) and BAIB (0.064 g, 0.20 mmol) were added and the reaction was left to stir at 0 °C overnight. After TLC analysis showed full conversion of the starting material the reaction was quenched by adding solid Na₂S₂O₃. The mixture was then further diluted with H₂O, acidified with AcOH and extracted with DCM thrice. The combined organic layers were washed with brine, dried over MgSO₄, filtered and concentrated *in vacuo*. The crude product was purified with flash silica column chromatography (pentane/acetone, 10:1→20:3 with 1% AcOH, v/v), to obtain the title compound (0.058 g, 0.065 mmol, 82%). ¹H NMR (400 MHz, CDCl₃): δ = 7.34 – 7.08 (m, 30H, 30CH Ar), 5.46 (d, *J* = 3.7 Hz, 1H, H-1'), 4.97 (d, *J* = 11.6 Hz, 1H, CHHPH), 4.89 (d, *J* = 10.9 Hz, 1H, CHHPH), 4.82 – 4.67 (m, 4H, 4CHHPH), 4.65 – 4.59 (m, 2H, 2CHHPH), 4.52 – 4.48 (m, 2H, 2CHHPH), 4.46 – 4.41 (m, 2H, 2CHHPH), 4.19 (t, *J* = 9.5 Hz, 1H), 3.94 (t, *J* = 9.4 Hz, 1H), 3.87 – 3.79 (m, 2H), 3.77 – 3.53 (m, 5H), 3.48 (dd, *J* = 9.9, 3.7 Hz, 1H), 3.21 – 3.18 (m, 1H, H-1/H-7, epoxide), 3.09 (d, *J* = 3.6 Hz, 1H, H-1/H-7, epoxide), 2.99 (dd, *J* = 9.3, 2.0 Hz, 1H, H-5) ppm. ¹³C NMR (101 MHz, CDCl₃): δ = 174.6, 139.1, 138.8, 138.4, 138.2, 138.0, 137.5 (7C_q), 129.2, 128.6, 128.5, 128.4, 128.3, 128.2, 128.1, 128.0, 127.8, 127.7, 127.6, 127.5, 127.2, 125.4 (19CH Ar), 97.8 (CH, C-1'), 83.0, 81.7, 79.7, 79.0, 77.7 (5CH), 75.7, 75.1, 74.8 (3CH₂), 74.5 (CH), 73.6, 73.3, 72.8 (3CH₂), 71.2 (CH), 68.5 (CH₂), 54.4 (CH, epoxide), 53.7 (CH, epoxide), 48.8 (CH, C-5) ppm. HR-MS (ESI): *m/z* calcd for C₅₅H₆₀O₁₁N⁺: 910.4161 [*M*+NH₄]⁺, found 910.4161.

Compound 3

Compound **20** (0.027 g, 0.030 mmol) was co-evaporated with anhydrous toluene thrice and dissolved in 1.25 mL anhydrous THF. *t*-BuOH (0.17 mL, 1.8 mmol) was added to this solution. Liquid ammonia was prepared fresh by cooling an empty round bottom flask to -60 °C while maintaining

a gentle gaseous flow of ammonia in the flask. Upon reaching the desired amount of liquid ammonia the flask was sealed off and placed under nitrogen atmosphere. Solid sodium (0.042 g, 1.8 mmol) was added to the liquid ammonia and the resulting solution turned blue. Compound **21** was added to the blue solution and the reaction was left to stir for 10 minutes. The reaction was quenched with AcOH (0.1 mL, 1.8 mmol) in H₂O (1 mL) after which the blue color disappeared. The reaction flask was transferred to a warm water bath and stirred for 30 minutes until all ammonia had evaporated. The remaining solution was concentrated in vacuo. The crude residue was purified using gel filtration to obtain compound **3** (0.0088 g, 0.024 mmol, 80%). ¹H NMR (850 MHz, D₂O): δ = 5.23 (d, *J* = 4.0 Hz, 1H, H-1'), 3.87 (d, *J* = 8.7, 0.8 Hz, 1H), 3.84 – 3.77 (m, 3H), 3.74 – 3.68 (m, 2H, H-3'), 3.59 – 3.57 (m, 1H), 3.54 (dd, *J* = 9.9, 4.0 Hz, 1H), 3.51 – 3.49 (m, 1H, H-7), 3.43 (t, *J* = 10.2, 9.2 Hz, 1H), 3.20 (d, *J* = 3.7 Hz, 1H, H-1, epoxide), 2.88 (dd, *J* = 9.7, 1.9 Hz, 1H, H-5) ppm. ¹³C NMR (214 MHz, D₂O): δ = 177.7 (C=O), 99.6 (CH, C-1'), 76.6, 76.2, 73.0, 71.8, 71.7, 70.7, 69.2 (7CH), 60.0 (CH₂, C-6'), 56.2 (CH, C-7, epoxide), 55.3 (CH, C-1, epoxide), 50.9 (CH, C-5) ppm. HR-MS (ESI): *m/z* calcd for C₁₃H₂₄O₁₁N⁺: 370.1344 [*M*+NH₄]⁺, found 370.1344.

3.6 References

- [1] B. Ernst, J. L. Magnani, *Nat. Rev. Drug Disc.* **2009**, *8*, 661–677.
- [2] R. J. Slack, R. Mills, A. C. Mackinnon, *Int. J. Biochem. Cell Biol.* **2021**, *130*, 105881.
- [3] R. Sommer, S. Wagner, K. Rox, A. Varrot, D. Hauck, E.-C. Wamhoff, J. Schreiber, T. Ryckmans, T. Brunner, C. Rademacher, R. W. Hartmann, M. Brønstrup, A. Imberty, A. Titz, *J. Am. Chem. Soc.* **2018**, *140*, 2537–2545.
- [4] M. von Itzstein, W. Y. Wu, G. B. Kok, M. S. Pegg, J. C. Dyason, B. Jin, T. Van Phan, M. L. Smythe, H. F. White, S. W. Oliver, P. M. Colman, J. N. Varghese, D. M. Ryan, J. M. Woods, R. C. Bethell, V. J. Hotham, J. M. Cameron, C. R. Penn, *Nature* **1993**, *363*, 418–423.
- [5] T. Cox, R. Lachmann, C. Hollak, J. Aerts, S. van Weely, M. Hrebíček, F. Platt, T. Butters, R. Dwek, C. Moyses, I. Gow, D. Elstein, A. Zimran, *Lancet* **2000**, *355*, 1481–1485.
- [6] L. K. Campbell, D. E. Baker, R. K. Campbell, *Ann. Pharmacother.* **2000**, *34*, 1291–1301.
- [7] M. von Itzstein, W. Y. Wu, G. B. Kok, M. S. Pegg, J. C. Dyason, B. Jin, T. Van Phan, M. L. Smythe, H. F. White, S. W. Oliver, P. M. Colman, J. N. Varghese, D. M. Ryan, J. M. Woods, R. C. Bethell, V. J. Hotham, J. M. Cameron, C. R. Penn, *Nature* **1993**, *363*, 418–423.
- [8] J. Enotarpi, M. Tontini, C. Balocchi, D. van der Es, L. Auburger, E. Balducci, F. Carboni, D. Proietti, D. Casini, D. V. Filippov, H. S. Overkleeft, G. A. van der Marel, C. Colombo, M. R. Romano, F. Berti, P. Costantino, J. D. C. Codeé, L. Lay, R. Adamo, *Nat. Commun.* **2020**, *11*, 4434.
- [9] S. Rivara, F. M. Milazzo, G. Giannini, *Future Med. Chem.* **2016**, *8*, 647–680.
- [10] C. D. Mohan, S. Hari, H. D. Preetham, S. Rangappa, U. Barash, N. Ilan, S. C. Nayak, V. K. Gupta, Basappa, I. Vlodavsky, K. S. Rangappa, *iScience* **2019**, *15*, 360–390.
- [11] F. Levy-Adam, S. Feld, V. Cohen-Kaplan, A. Shteingauz, M. Gross, G. Arvatz, I. Naroditsky, N. Ilan, I. Doweck, I.

- Vlodavsky, *J. Biol. Chem.* **2010**, *285*, 28010–28019.
- [12] I. Vlodavsky, Y. Friedmann, M. Elkin, H. Aingorn, R. Atzmon, R. Ishai-Michaeli, M. Bitan, O. Pappo, T. Peretz, I. Michal, L. Spector, I. Pecker, *Nat. Med.* **1999**, *5*, 793–802.
- [13] U. Barash, V. Cohen-Kaplan, I. Dowek, R. D. Sanderson, N. Ilan, I. Vlodavsky, *FEBS J.* **2010**, *277*, 3890–3903.
- [14] J. P. Ritchie, V. C. Ramani, Y. Ren, A. Naggi, G. Torri, B. Casu, S. Penco, C. Pisano, P. Carminati, M. Tortoreto, F. Zunino, I. Vlodavsky, R. D. Sanderson, Y. Yang, *Clin. Cancer Res.* **2011**, *17*, 1382–1393.
- [15] M. Chhabra, V. Ferro, *Adv. Exp. Med. Biol.* **2020**, *1221*, 473–491
- [16] K. Dredge, T. V. Brennan, E. Hammond, J. D. Lickliter, L. Lin, D. Bampton, P. Handley, F. Lankesheer, G. Morrish, Y. Yang, M. P. Brown, M. Millward, *Br. J. Cancer* **2018**, *118*, 1035–1041.
- [17] H. Zhou, S. Roy, E. Cochran, R. Zouaoui, C. L. Chu, J. Duffner, G. Zhao, S. Smith, Z. Galcheva-Gargova, J. Karlgren, N. Dussault, R. Y. Q. Kwan, E. Moy, M. Barnes, A. Long, C. Honan, Y. W. Qi, Z. Shriver, T. Ganguly, B. Schultes, G. Venkataraman, T. K. Kishimoto, *PLoS One* **2011**, *6*, e21106.
- [18] A. MacDonald, M. Priess, J. Curran, J. Guess, V. Farutin, I. Oosterom, C. L. Chu, E. Cochran, L. Zhang, K. Getchell, M. Lolkema, B. C. Schultes, S. Krause, *Mol. Cancer Ther.* **2019**, *18*, 245–256.
- [19] V. Masola, G. Zaza, G. Bellin, L. Dall'Olmo, S. Granata, G. Vischini, M. F. Secchi, A. Lupo, G. Gambaro, M. Onisto, *FASEB J.* **2018**, *32*, 742–756.
- [20] I. O. Koliesnik, H. F. Kuipers, C. O. Medina, S. Zihlsler, D. Liu, J. D. van Belleghem, P. L. Bollyky, *Front. Immunol.* **2020**, *11*, 1–14.
- [21] C. de Boer, Z. Armstrong, V. A. J. Lit, U. Barash, G. Ruijgrok, I. Boyango, M. M. Weitzberg, S. P. Schröder, A. J. C. Sarris, N. J. Meeuwenoord, P. Bule, Y. Kayal, N. Ilan, J. D. C. Codée, I. Vlodavsky, H. S. Overkleeft, G. J. Davies, L. Wu, *Proc. Natl. Acad. Sci. U.S.A.* **2022**, *119*, e2203167119.
- [22] L. Wu, J. Jiang, Y. Jin, W. W. Kallemeijn, C.-L. Kuo, M. Artola, W. Dai, C. van Elk, M. van Eijk, G. A. van der Marel, J. D. C. Codée, B. I. Florea, J. M. F. G. Aerts, H. S. Overkleeft, G. J. Davies, *Nat. Chem. Biol.* **2017**, *13*, 867–873.
- [23] Y. Nishimura, T. Kudo, S. Kondo, T. Takeuchi, *J. Antibiot.* **1994**, *47*, 101–107.
- [24] Y. Nishimura, E. Shitara, H. Adachi, M. Toyoshima, M. Nakajima, Y. Okami, T. Takeuchi, *J. Org. Chem.* **2000**, *65*, 2–11.
- [25] J. W. Woollen, P. G. Walker, *Clin. Chim. Acta* **1965**, *12*, 659–670.
- [26] M. F. Dean, J. C. Martin, *Biochem J.* **1988**, *256*, 335–341.
- [27] P. B. Jariwala, S. J. Pellock, D. Goldfarb, E. W. Cloer, M. Artola, J. B. Simpson, A. P. Bhatt, W. G. Walton, L. R. Roberts, M. B. Major, G. J. Davies, H. S. Overkleeft, M. R. Redinbo, *ACS Chem. Biol.* **2020**, *15*, 217–225.
- [28] R. M. Pollet, E. H. D'Agostino, W. G. Walton, Y. Xu, M. S. Little, K. A. Biernat, S. J. Pellock, L. M. Patterson, B. C. Creekmore, H. N. Isenberg, R. R. Bahethi, A. P. Bhatt, J. Liu, R. Z. Gharaibeh, M. R. Redinbo, *Structure* **2017**, *25*, 967–977.
- [29] X. Cheng, N. Khan, D. R. Mootoo, *J. Org. Chem.* **2000**, *65*, 2544–2547.
- [30] C.-F. Liu, *Molecules* **2022**, *27*, 7439.
- [31] L. Clarion, C. Jacquard, O. Sainte-Catherine, M. Decoux, S. Loiseau, M. Rolland, M. Lecouvey, J.-P. Hugnot, J.-N. Volle, D. Virieux, J.-L. Pirat, N. Bakalara, *J. Med. Chem.* **2014**, *57*, 8293–8306.
- [32] H. Driguez, *Chembiochem.* **2001**, *2*, 311–318.
- [33] A. W. McDonagh, M. F. Mahon, P. V. Murphy, *Org. Lett.* **2016**, *18*, 552–555.
- [34] R. Eskandari, K. Jayakanthan, D. A. Kuntz, D. R. Rose, B. M. Pinto, *Bioorg. Med. Chem.* **2010**, *18*, 2829–2835.
- [35] D. L. Zechel, A. B. Boraston, T. Gloster, C. M. Boraston, J. M. Macdonald, D. M. G. Tilbrook, R. V. Stick, G. J. Davies, *J. Am. Chem. Soc.* **2003**, *125*, 14313–1423.
- [36] Q. Gao, C. Zaccaria, M. Tontini, L. Poletti, P. Costantino, L. Lay, *Org. Biomol. Chem.* **2012**, *10*, 6673–6681.
- [37] S. P. Schröder, W. A. Offen, A. Males, Y. Jin, C. de Boer, J. Enotarpi, L. Marino, G. A. van der Marel, B. I. Florea, J. D. C. Codée, H. S. Overkleeft, G. J. Davies, *Chem. Eur. J.* **2021**, *27*, 9519–9523.

- [38] F. G. Hansen, E. Bundgaard, R. Madsen, *J. Org. Chem.* **2005**, *70*, 10139–10142.
- [39] T. P. Ofman, F. Küllmer, G. A. van der Marel, J. D. C. Codée, H. S. Overkleeft, *Org. Lett.* **2021**, *23*, 9516–9519.
- [40] D. R. Mootoo, P. Konradsson, U. Udodong, B. Fraser-Reid, *J. Am. Chem. Soc.* **1988**, *110*, 5583–5584.
- [41] J. B. Epp, T. S. Widlanski, *J. Org. Chem.* **1999**, *64*, 1, 293–295.
- [42] L. Wu, C. Viola, A. Brzozowski, G. J. Davies, *Nat. Struct. Mol. Biol.* **2015**, *22*, 1016–1022.
- [44] Y. Chen, Z. Armstrong, M. Artola, B. I. Florea, C.-L. Kuo, C. de Boer, M. S. Rasmussen, M. A. Hachem, G. A. van der Marel, J. D. C. Codée, J. M. F. G. Aerts, G. J. Davies, H. S. Overkleeft, *J. Am. Chem. Soc.* **2021**, *143*, 2423–2432.

